Small Unmanned Aerial Vehicle System for Wildlife Radio Collar Tracking

Gilberto Antonio Marcon dos Santos[1], Zachary Barnes[2], Eric Lo, Bryan Ritoper, Lauren Nishizaki, Xavier Tejeda[2], Alex Ke, Han Lin, Curt Schurgers, Albert Lin and Ryan Kastner
University of California, San Diego
gilbertoantoniomarcon@gmail.com, zab25@pitt.edu, eklo@ucsd.edu, britoper@gmail.com, lnishizaki@hmc.edu, tejedax12@gmail.com, ayke@ucsd.edu, han.w.lin@aero.org, cschurgers@ucsd.edu, kastner@ucsd.edu

***Abstract*—This paper describes a low cost system for tracking wildlife that is equipped with radio collars. Currently, researchers have to physically go into the field with a directional antenna to try to pinpoint the VHF (very high frequency) signal originating from a wildlife tracking collar. Depending on the terrain, it could take an entire day to locate a single animal. To vastly improve upon this traditional approach, the system proposed here utilizes a small fixed-wing aircraft drone with a simple radio on-board, flying an automated mission. Received signal strength is recorded, and used to create a heat map that shows the collar's position. A prototype of this system was built using off-the-shelf hardware and custom signal processing algorithms. Initial field tests confirm the systems capabilities and its promise for wildlife tracking.**

Keywords—Radio Tracking; Wildlife Telemetry; Small Unmanned Aerial Vehicles; Software-Defined Radio; Digital Signal Processing

I. INTRODUCTION

A common way to achieve wildlife tracking is using radio collars. This system consists of a transmitter (the radio collar) and a receiving system (a hand-held directional antenna), both operating on the very high frequency (VHF) spectrum range [1]. This method has been the most common telemetry approach in the field since its first workable system, described in [2]. Compared to the other common telemetry techniques (satellite tracking and Global Positioning System, GPS), VHF presents the lowest initial cost, the longest life cycle and the smallest form-factor collars. Its greatest downside is its labor intensiveness requirement, since tracking is typically done on foot, carrying a directional portable antenna and listening to the received signal (see Fig. 1). Eliminating the labor-intensive side of the method would greatly benefit wildlife research, enabling the gathering of much broader amounts of data and covering vaster areas [1].

Fig. 1. Traditional VHF tracking approach.

Presenting a new approach for VHF radio collar tracking using low cost off-the-shelf components is the goal of this work. Specifically, we will leverage the emergence of low-cost aerial drones and simple-yet-flexible programmable radio technologies to create a powerful new system. Simulations and field data prove its potential as a viable substitute for the current method in a diverse set of scenarios.

A. Conventional Wildlife Radio-Tracking and its Limitations

Most of the radio transmitting collars used in wildlife research operate in the 148-152 MHz, 163-165 MHz, and 216-220 MHz ranges, which provides a good balance between antenna size (due to wavelength) and propagation effectiveness on the wilderness. Each radio collar transmits at a single frequency, with a drift of around 1~2 kHz depending on temperature and battery conditions. The frequencies of different collars are tuned at least at 10 kHz apart for distinctiveness. To extend battery life, most collars transmit pulses intermittently, usually 30 to 120 times per minute, with each pulse as short as 18 milliseconds [1].

The goal of our system is to be able to track these legacy radio collars, but replace the hand-held directional system with an automated aerial vehicle. In addition to the inherent gain of flying over an area of interest instead of walking through it, our proposed aerial system is also capable of tracking multiple collars at the same time, but relying on a software-defined-radio (SDR).

The reason why we are able to build such a system (aerial fixed wing drone with a software defined radio), at a reasonable cost, is that the relevant technologies have recently moved into the consumer space.

This work was supported by NSF Grant 1263320 and by the San Diego Zoo. [1]The work of The work of (1) was supported by the CAPES Foundation, Brazil. [2]The work of (2) was supported by the NSF REU Program.

B. Enabling Technologies

Advances in low cost platforms often ride the wave to consumer electronics. Technologies designed for the consumer space benefit from the economies of scale, often resulting in a significant drop in prices, not only of the end product, but also of the constituent component technologies. Two technologies that have experienced this proliferation and resulting drop in price and increase in availability, and that are particularly relevant for our project are digital television dongle receivers and small unmanned aerial (UAV) vehicles for hobbyists (more commonly known as "drones").

Digital television receivers, for example, have made programmable radios readily accessible at low costs. Their receiver chain hardware is much the same as that of a generic Software-Defined Radio (SDR), containing a Low Noise Amplifier (LNA), a Software-Controlled Demodulator and an Analog to Digital Converter (ADC). However, the relative cost a TV receiver dongle compared to a purpose-made SDR of similar specs is one order of magnitude lower, thus making the software controllable TV receiver an attractive option for developing low cost SDR applications, which is one of the key components of our system.

Similarly, hobby UAV technology has benefitted from the proliferation of low cost sensors and microcontrollers in consumer electronics. Leveraging readily accessible sensors, combined with powerful microcontrollers, hobbyists have created fully autonomous platforms capable of waypoint navigation without intervention from a human pilot. This opens up the possibility of deploying sensors in the air at a significantly lower cost compared to manned aviation.

II. Proposed System

A. System Model

Our proposed aerial system for radio collar tracking consists of a small UAV carrying a Global Positioning System (GPS) unit, a low cost television receiver dongle serving as an SDR unit attached to an omnidirectional antenna, a programmable control board for command and data storage and the relevant software for after-flight data processing. The flight path is intended to follow a lawnmower pattern, covering evenly the entire search area. During the flight, the control board interfaces with the radio, and records the raw downconverted signals from the SDR as well as the GPS data. The use of an omnidirectional antenna simplifies the overall system operation, since it does not requires accounting precisely for the plane orientation during flight or deploying an accurate control system for directing the antenna. Fig. 2 presents an example of a lawnmower flight pattern.

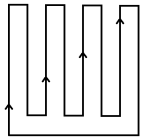

Fig. 2. Example of a lawnmower flight pattern.

B. Frequency Ranges and File Protocol

In order to make the system as general as possible, capable of operating with the widest range of collars and conditions, all the key parameters were made available for the end user to define as a configuration file. Such parameters are listed below:

- Demodulator center frequency;
- ADC bandwidth (sampling frequency, F_s);
- Expected collar pulse duration;
- Expected collar pulse periodicity (How often the pulse is transmitted); and
- Expected collar frequency accuracy, or Frequency Error Margin (FEM).

Different SDR devices will restrict those parameters to different ranges, specially the first two parameters, since they relate directly to the demodulator and the ADC architecture. The other three parameters are associated with the way the signal is framed and processed, not being restricted by any hardware limits, to the extent of the present application.

The proposed system chops the input signal in equal sized blocks, having a time length equivalent to the radio collar pulse duration, which ranges from 0.5 to 2 seconds in most radio collars. The SDR provides both the real and imaginary (its quadrature-modulated counterpart) parts of a signal, and both are stored and used in the post-processing.

Each time-frame signal block is stored, along with the frame corresponding GPS positioning (the given GPS position at the time when the VHF signal was captured). In order to provide good performance in recording big amounts of data in real time, we used a binary file format, and a limited number of frames are stored per file to provide good file manageability. The diagram for the file format proposed is presented in Fig. 3.

2xSampling Frequency bytes	1 byte	12 bytes
Demodulated signal frame 1	Current Analog Gain	GPS pos.
Demodulated signal frame 2	Current Analog Gain	GPS pos.
Demodulated signal frame 3	Current Analog Gain	GPS pos.
	...	
Demodulated signal frame n	Current Analog Gain	GPS pos.

Fig. 3. Proposed file format for storing collected data in-flight.

C. Post-Processing

The actual data processing is done in post-processing, after the UAV has landed and the stored data extracted. This provides mainly three advantages: (a) flexibility for the researcher to adopt solely one part or the whole system, according to his needs; (b) allows to the user develop their own version of the post-processing part and (c) enables long term improvement in the data processing methods, once it will be available for future approaches and experimentation.

The key element in the data processing part of the system is the algorithm that detects the pings from the radio collar in the received (noisy) signal. Since the pings are of predefined known duration, the processing operates on fixed sized blocks

of data, of a length corresponding to these pings. A Fast Fourier Transform (FFT) is executed over each block/window, generating a frequency domain representation. The signal strength at the collar pulse frequency corresponding bin is evaluated and stored in an auxiliary array. That value is associated to the window starting position over the whole frame. This method essentially evaluates the signal strength for the specific collar frequency at different windowing positions of the frame. In other words, it looks for the best position to slice over each frame, better framing the signal burst emitted by the collar. To achieve this, FFTs are applied over different time slices of a signal frame, generating its time–frequency representation. Such representation is shown in Fig. 4 for a synthesized signal in the presence of Additive White Gaussian Noise (AWGN). The frame length is of 4000 samples and the window length is of 400 samples, allowing for 3600 unique windowing positions, all of which are presented on the plot.

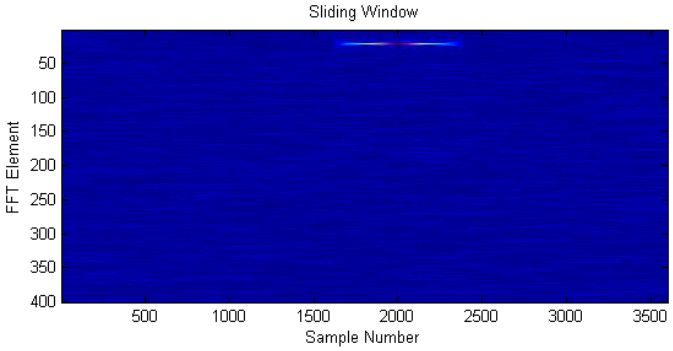

Fig. 4. FFTs taken from a signal frame for different slicing positions. The sinusoidal pulse is clearly visible at the top of the plot. The Signal to Noise Ratio (SNR) is of 10 dB.

After the algorithm loops through the whole frame and the most appropriate window is selected, the signal and the noise spectral power are calculated. For that matter a final FFT is calculated. The squared value of the expected signal bin is taken as the signal power and the power of the remainder spectrum is taken as noise power. The Signal-to-Noise Ratio (SNR) is then calculated as in (1).

$$SNR = \mathrm{P}_{\text{signal bin}} / \mathrm{P}_{\text{remainder spectrum bins}} \quad (1)$$

For each frame a SNR value is to be associated with the current GPS position and those are then kept for the last processing step. Fig. 5 presents how the value at the pulse frequency bin varies as we window in different positions of the frame. It is assumed that, the higher this value is, the more likely it is that the algorithm framed exactly over the pulse. The analyzed signal is the same for Fig. 4.

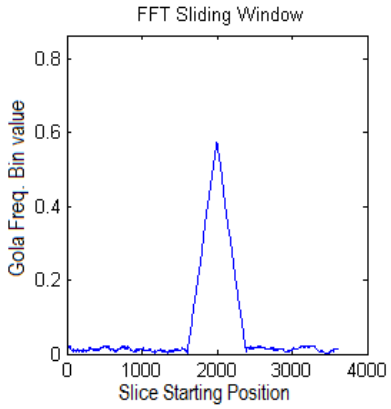

Fig. 5. Value read at a specific FFT bin for different windowing starting positions. The peak represents the windowing position at which the frame is fully aligned with the pulse.

For most cases, the FFT will provide greater frequency resolution than the expected collar pulse accuracy (which ranges from 1 to 2 MHz, depending on temperature and battery). The FFT frequency resolution relates directly to the number of samples of the provided array. The higher the number of samples provided, the higher the number of frequency bins. Thus, the collar-emitted pulse may not fall in the expected FFT bin, calculated by the nominal collar frequency. This must be taken into account for implementation purposes. Not only the nominal bin shall be evaluated during the FFT runs, but all the range of bins at which the pulse may show up must be evaluated. This range is calculated based on the collar frequency error margin, an additional parameter made available for the end user. Every time the system evaluates FFT signal strength it will run through the whole frequency range and take the greatest-value bin as the corresponding "correct window likelihood".

After all the flight raw data is evaluated, the signal strength/positioning information is then used to plot a heat map over the flight area, representing how strong was the signal over each location. This heat map is the final product of the system, providing the user with an accurate map of signal strength for each collar searched.

III. Method Validation through Prototyping

A prototype system was implemented in order to test and validate the proposed architecture. By the time this paper was written the GPS integration was still under development, therefore the post-SNR calculation section of the system is not detailed here. The following sections present the low cost off-the-shelf components adopted and the hardware and software implementation details of the set-up followed by the simulated and field test procedures.

A. Hardware

For the hardware portion of the system, a generic digital television receiver dongle was used as an SDR, as it is the lowest cost and form factor device capable of providing basic software-programmable SDR functionality available on the market. A Texas Instruments BeagleBone Black (BBB) board

was adopted as the main control broad, due to its capability of running a fully functional Linux operating system (OS) meeting a basic personal computer performance requirements; and a high capacity (64 GB) Secure Digital (SD) card as main data storage device due to its reduced form factor, cost and power requirements. Fig. 6 presents a block diagram of the hardware-side of the system implemented.

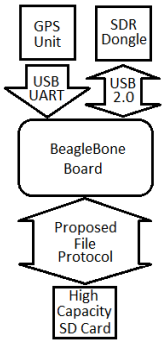

Fig. 6. Simplified hardware diagram of the system, as it is itended to be deployed on a small UAV.

The receiver dongle has a Universal Serial Bus (USB) 2.0 as its communication port, which is used as the communication interface with the BBB. It contains a Rafael Micro R820T tuner capable of demodulating complex signals at carriers ranging from 24 MHz to 1766 MHz and a two-channel 8-bits ADC capable of operating at sampling frequencies of up 2.4 MHz, providing real and imaginary (quadrature) signals.

B. *Software*

For the software-hardware interface, the RTL-SDR library, an open-source reverse-engineered software interface for the hardware, was chosen since no official Application Programming Interface (API) or datasheet is openly provided by the dongle Integrated Circuit (IC) makers. A C-language code program based on the RTL-SDR API was implemented to run on the BBB Linux. The program deals with reading GPS positioning data and recording the demodulated signals from the dongle on the SD card.

Having each frame captured every 1.5 seconds, sampled at 2 MHz and quantized at 8-bits for both real and imaginary signals, generates 6 Megabytes of data per frame. Four frames are kept per file, generating 24 Megabytes files every 6 seconds, 240 Megabytes of data per minute and 14.4 Gb per hour. Under those circumstances, one SD card can store up to 4 hours of raw data, providing plenty of run time for the system (as the typical maximum flight time of our platform is in the range of an hour).

C. *Simulation Procedures*

Two different metrics were devised to quantify the simulation results of the post-processing method. The first consists of simply checking whether the system windowed the signal in the correct place (framing exactly the pulse) within an error margin of 1/3 of the pulse length. Synthetic data is generated and fed to the system and the correct windowing position is compared with the one obtained by the algorithm. A Frame Detection Error Rate (FDER) is calculated for decreasing SNR values. The second metric consists of feeding the system with the very same synthetic signal input as for the first metric and then comparing the actual SNR with the SNR that the system calculates. The following parameters were adopted for all simulations:

- Pulse frequency: 2.000 kHz;
- SNR ranging from 10.0 dB to -40.0 dB;
- 100 different frames per SNR value;
- Signal frame duration of 1.5 seconds; and
- Pulse duration is of 20 milliseconds.

D. *Field Test Procedures*

For verifying the consistency of the calculated SNR, the system was deployed on a multirotor UAV. Data was collected while keeping a collar on ground, fixed at a specific position during each flight. Two different paths were used: a vertical path, having the UAV take off above the collar position, ascending over 100 meters and descending vertically; and a horizontal path, having the UAV to ascend 30 meters vertically from the collar position, translate horizontally 240 meters and return through the same path, descending vertically and finally landing over the collar. Additionally, for the vertical path, the UAV shall ascend in steps, loitering approximately every 5 meter ascended so that a reasonable amount of data is recorder during ascension.

It is important to remark, though, that the main goal of this test procedure is not to accurately measure the SNR at every single instant for each run, but to attest the overall consistency of the SNR values measured. This way, the precise positions of each climbing step are not essential as the overall system scheme does not relies on individual SNR measurements, but on the general consistency of the measurements for ultimately composing a SNR heat map across the search area.

IV. Results

A. *Simulation Results*

For comparing the overall system performance under relevant combinations of parameters and sampling frequencies, six simulation instances were executed, each having different parameters, all of which are detailed on table I.

TABLE I. EXECUTED SIMULATIONS

Simulation Run	***Frequency Error Margin (Hz)***	***Sampling Frequency (kHz)***
a	***1500.0***	***10.240***
b	***500.0***	***10.240***
c	***150.0***	***10.240***
d	***1500.0***	***40.960***
e	***500.0***	***40.960***
f	***150.0***	***40.960***

Both Frame Detection Error Rate and Measured SNR versus Actual SNR metrics and two different sampling frequencies were used: 10.240 and 40.960 Hz. Those frequencies were chosen for oversampling the signal in more than five times and for being sufficiently distant. For each frequency, tree different values for the "frequency error margin" parameter were tested: 150, 500 and 1500 Hz. The results of the six runs are presented in Fig. 7.

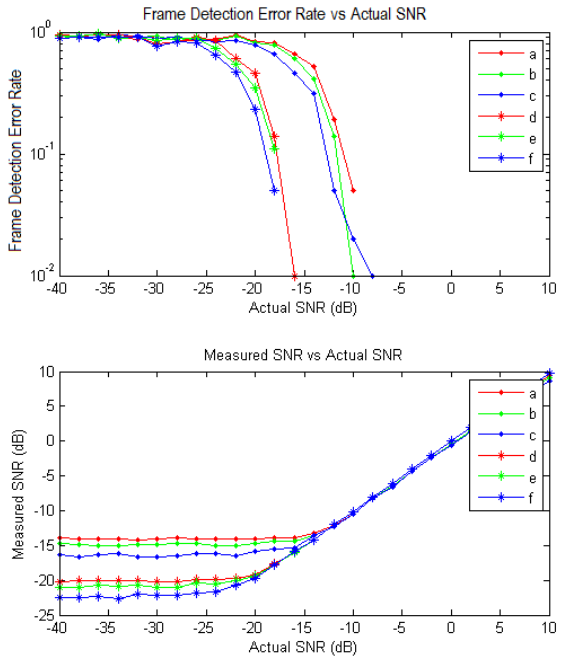

Fig. 7. Simulation results: (a) F_s = 10.240 kHz, FEM = 1500.0 Hz; (b) F_s = 10.240 kHz, FEM = 500.0 Hz; (c) F_s = 10.240 kHz, FEM = 150.0 Hz; (d) F_s = 40.960 kHz, FEM = 1500.0 Hz; (e) F_s = 40.960 kHz, FEM = 500.0 Hz; (f) F_s = 40.960 kHz, FEM = 150.0 Hz;

From those results, it is clear that, keeping all the other parameters constant, increasing the sampling rate will decrease the FDER. This is due to the fact that the increase in sampling rate will cause an increase in the overall number of samples, providing for more FFT bins. The more FFT bins, the more frequency resolution it provides, making it easier to distinguish the specific signal from noise and thus decreasing the likelihood of windowing off the signal burst.

On the other hand, decreasing the FEM also decreases the FDER. Making it smaller tells the algorithm to consider a narrower frequency band as potential signal source, thus making it less susceptible to mix signal and noise. There is a tradeoff for this parameter though, since the actual collar frequency certainty is limited. This frequency is susceptible to change depending on various external factors. This said, the narrower the FEM, the more accurate the system, but also the greater the chances of completely missing the signal for it not being within the defined range.

Comparing values closely one can tell that by increasing the sampling frequency four times, the actual SNR value for a given FDER is reduced in 6 dB, which is approximately 4 times. By that measure, one concludes then that the relationship between F_s and the SNR bottom is approximately linear and proportional. Thus, it would be expected that, in an ideal AWGN environment, increasing F_s by a factor of 100 would also lower the SNR floor by 20 dB.

From the second plot it is noticeable that FDER is directly associated with how well the measured and the actual SNR correlate. A higher FDER will increase the likelihood of treating noise as signal and thus calculating wrong SNR values. This plot also shows that by increasing sampling rate and decreasing FEM, the range of SNR cases for which the system will give accurate measurements will get wider, increasing thus the overall signal detection range.

B. Field Test Results

The two different proposed field tests were executed. The following parameters are common for both tests:

- Sampling Frequency 2.048 MHz
- Collar frequency: 172.742 MHz;
- Demodulator Frequency: 172.600 MHz;
- Signal frame duration is of 1.5 seconds; and
- Pulse duration is of 20 milliseconds.

The calculated SNR values for each test are presented in Fig. 8 and Fig. 9. All the values are plotted, including those preceding takeoff and succeeding landing. It is important to remark that for those two situations, the receiver antenna is amidst ground grass for it was attached to the vehicle ground support. Thus, the reception at those points was vastly influenced and those readings are not relevant for the overall evaluation of the system performance for tracking purposes.

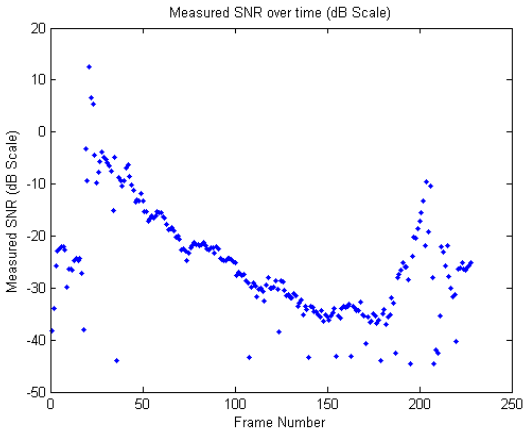

Fig. 8. Vertical path field test: SNR per time frame F_s = 2.048 MHz.

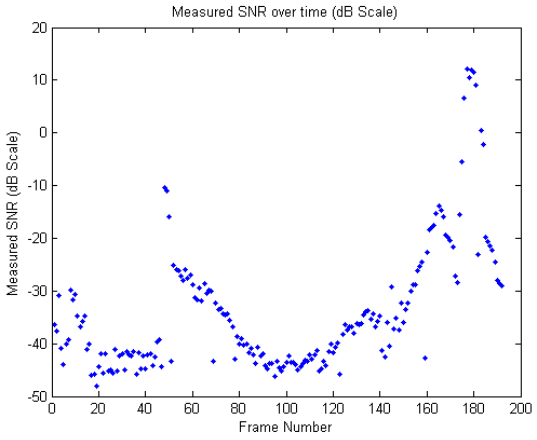

Fig. 9. Horizontal path field test: SNR per time frame F_s = 2.048 MHz.

For the 10.024 kHz sampling frequency adopted for one of the simulations we concluded that the SNR floor would be below -15 dB (Fig. 7). For the adopted F_s of 2.048 MHz in the field tests, the theoretical SNR floor would then be 23 dB under, since it is 200 times greater than the simulated F_s. This gives us, then, a theoretical signal detection floor of -38 dB. This means that for any signal having a SNR lesser than -38 dB the FDER will jeopardize the SNR detection accuracy. As we can tell from Fig. 7, all values laying bellow that margin will result in measured SNRs of a few units bellow -38 dB. This is exactly what we observe from plots in Fig. 8 and Fig. 9, where no measurement is much lesser than -38 dB (the noise floor). All values bellow that mark shall be interpreted as absence of signal.

An important observation about the presented data is that, depending on the granularity of the FFT, the collar signal may be spread through many frequency bins, instead of just one. This affects the SNR calculation for the present algorithm, since it will solely consider the single greatest bin in the valid range, ignoring its neighboring bins and thus much of the actual signal, depending on the granularity. This does not affect the overall system consistency, though, since the granularity is constant for a given run. The only effect is that of a uniform scale of all values for a single run.

For each plot, the frames captured while the vehicle was on ground are easily noticed. The contact with ground significantly obstructs the receiver antenna attenuating the signal in approximately four orders of magnitude in those examples. A few outliers can also be spotted throughout the plots resting at the bottom, most of them as the lowest values of each plot. Those outliers are due to the lack of synchronization between the transmitted pulse bursts and the receiver framing and the fact that the collar duty cycle period does not matches exactly it nominal value. Occasionally, then, some frames will not contain any signal burst and the SNR calculated will reach the noise floor. Having a slightly longer frame time would potentially be a simple solution for this issue.

The measured SNR values decay exponentially, as expected, as transmitter and receiver are displaced further away. The overall displacement of the points is coherent and compatible with the path executed by the UAV. For the first plot, it is clear that the ascending part of the course took longer than the descending part. The vehicle ascended in steps, which are also clear on the plot, and descended straight. For both runs the noise bottom was not reached during flight, given that throughout the plots, all values, to the exception of the outliers, are consistent with the constantly moving state of the plane (either getting away or closer to the collar).

Given the above, an UAV flying at an average altitude of 30 meters from the ground could detect signals at a radius of, at least 240 meters, making the overall system a potentially viable substitute for the current method using the low cost hardware adopted for the described implementation. As an addition, since a single flight can cover a vast area in less than an hour, subsequent flights may be performed as necessary, over a more specific area, refining the initial approximation with more precise data. Another possibility is that of using the SDR-UAV as an initial approach, skimming over a vast area and providing initial insight about the animal position. The researcher, then, will have a much more restricted area to scan manually, using the conventional VHF method. Either approach provides potentially large improvement in reducing the time and labor currently required to track animals in the field.

V. Conclusion

Both the simulation and the field results have demonstrated the potential for the method as an effective substitute for the conventional “on foot” VHF radio tracking. The synthetic tests proved the post processing approach to be effective even under challenging noise environments (a way under 0 dB, depending on sampling frequency). There are still big challenges to face, though, concerning the many inaccuracies caused by the low cost radio adopted. Such challenges may be overcome with the adoption of a higher end radio or further investigations over the reverse-engineered API available for the present device. Ultimately, at the present state of implementation, the prototype have demonstrated the method to be a promising low cost and fast to deploy solution, to be used either alone or combined with the conventional VHF method for wildlife tracking.

Acknowledgment

The authors would like to thank the San Diego Zoo for providing valuable support, insight and the specific hardware that is currently used for VHF tracking. This work was funded in part by NSF REU Site: Engineers for Exploration, Grant #1263320.

References

[1] L. D. Mech and S. M. Barber, “A critique of wildlife radio-tracking and its use in national parks : a report to the National Park Service,” U.S. Geological Survey, Northern Prairie Wildlife Research Center. Jamestown, N.D., 2002.

[2] W. W. Cochran and R. D. Lord Jr. 1963. A radio-tracking system for wild animals. J. Wldl. Manage. 27:9-24.